



## OPEN ACCESS

## EDITED BY

Karoly Nemeth,  
Institute of Earth Physics and Space  
Sciences, Hungary

## REVIEWED BY

Francesco Mazzarini,  
Istituto Nazionale di Geofisica e  
Vulcanologia (INGV), Italy  
Gabriel Ureta,  
National Research Center for Integrated  
Natural Disaster Management (CIGIDEN),  
Chile

## \*CORRESPONDENCE

Melanie Sieburg,  
✉ melanie@sieburg-shs.de

RECEIVED 19 February 2023

ACCEPTED 18 April 2023

PUBLISHED 10 May 2023

## CITATION

Sieburg M, Gernon TM, Keir D, Bull JM,  
Taylor RN, Watts EJ, Greenfield T and  
Gebru EF (2023), Temporal clustering of  
fissural eruption across multiple  
segments within the Ethiopian Rift.  
*Front. Earth Sci.* 11:1169635.  
doi: 10.3389/feart.2023.1169635

## COPYRIGHT

© 2023 Sieburg, Gernon, Keir, Bull,  
Taylor, Watts, Greenfield and Gebru. This  
is an open-access article distributed  
under the terms of the [Creative  
Commons Attribution License \(CC BY\)](https://creativecommons.org/licenses/by/4.0/).  
The use, distribution or reproduction in  
other forums is permitted, provided the  
original author(s) and the copyright  
owner(s) are credited and that the original  
publication in this journal is cited, in  
accordance with accepted academic  
practice. No use, distribution or  
reproduction is permitted which does not  
comply with these terms.

# Temporal clustering of fissural eruption across multiple segments within the Ethiopian Rift

Melanie Sieburg<sup>1,2\*</sup>, Thomas M. Gernon<sup>1</sup>, Derek Keir<sup>1,3</sup>,  
Jonathan M. Bull<sup>1</sup>, Rex N. Taylor<sup>1</sup>, Emma J. Watts<sup>1</sup>,  
Tim Greenfield<sup>4</sup> and Ermias F. Gebru<sup>5,6</sup>

<sup>1</sup>School of Ocean and Earth Science, University of Southampton, Southampton, United Kingdom, <sup>2</sup>Landesamt für Geologie und Bergwesen Sachsen-Anhalt, Halle (Saale), Germany, <sup>3</sup>Dipartimento di Scienze della Terra, University of Florence, Florence, Italy, <sup>4</sup>Department of Earth Sciences, University of Cambridge, Cambridge, United Kingdom, <sup>5</sup>Department of Geosciences, University of Fribourg, Fribourg, Switzerland, <sup>6</sup>School of Earth Sciences, Addis Ababa University, Addis Ababa, Ethiopia

Magmatic continental rifts show evidence that discrete rift segments experience episodic intrusive and eruptive events, more commonly termed rifting episodes. However, whether multiple rifting episodes across adjacent rift segments are clustered in time is not well understood. To address this issue, we conduct new radiocarbon dating that constrains the timing of the most recent rifting episode at the Boset magmatic segment of the northern Ethiopian rift, and combine this with historical dating of similar rifting events in the adjacent magmatic segments. New radiocarbon dates of multiple charcoal samples from the base of the most recent fissural lava at the Boset Volcanic Complex indicate that it likely occurred between 1812 and 1919 CE. These dates are similar to those from historical accounts of fissural eruption from the neighbouring Kone (~1810 CE), and Fantale (~1770 to 1808 CE) magmatic segments. We conduct new analysis of major and trace element compositions from these historical fissural lavas, as well as from a fresh-looking lava flow from Beru cone near to Kone volcano. The results of the geochemistry from these flows of all three magmatic segments show compositions that vary in the basalt and trachybasalt fields, with sufficient variation to rule out them having erupted from a single dike intrusion episode. This, combined with the scatter in dates from the radiocarbon analysis and historical accounts, along with the location of each eruption in a discrete and spatially offset magmatic segment, favours an interpretation of each magmatic segment experiencing separate rifting episodes but with these being clustered in time. Mechanisms to explain the clustering of rifting episodes are more speculative but could include stress transfer from dike intrusion and deep crustal hydraulic connection in the plumbing system of multiple segments.

## KEYWORDS

radiocarbon dating (<sup>14</sup>C) of charcoal, Main Ethiopian Rift, Boset-Bericha Volcanic Complex, temporal clustering of volcanic eruptions, mafic fissure eruption, Kone Volcano, Fantale Volcano

## 1 Introduction

Magma-rich continental rifts extend by a combination of faulting and magma intrusion (e.g., Ebinger and Casey, 2001). While the time-averaged, far field plate motions are well constrained, using, for example, GPS measurements and tectonic plate reconstructions (e.g., Viltres et al., 2020), the variability of magmatic and tectonic processes in space and time at the plate boundary is poorly constrained. The East African Rift System (EARS), one of the most tectonically and volcanically active regions on Earth, is gradually extending the African continent. In the Main Ethiopian Rift (MER), the northern portion of the EARS, the majority of extension and volcanism is concentrated within in-rift magmatic segments defined by relatively short and small-offset fault systems that cut rift-parallel volcanic ranges with aligned chains of volcanic cones and fissural flows (Ebinger and Casey, 2001; Siegburg et al., 2020) (Figure 1). These magmatic segments (e.g., the Boset magmatic segment) are similar in size, morphology, structure, and spacing to the second-order non-transform segments of slow-spreading mid-ocean ridges (Hayward and Ebinger, 1996; Carbotte et al., 2016; Siegburg et al., 2020).

Observations such as seismicity and geodesy of modern-day rifting episodes in Ethiopia and Iceland suggest the crust of individual magmatic segments rupture independently during discrete rifting episodes involving upper crustal dike, dike-induced seismicity, and dike-fed fissural lava flows (e.g., Wright et al., 2006; Sigmundsson et al., 2015; 2022; Barnie et al., 2016). During these rifting episodes, metre to several metre-wide dike intrusion accommodates several decades to centuries of extensional strain accumulation in elastic crust (Pagli et al., 2015). As a result,

rifting episodes in single magmatic segments tend to be temporally spaced at repeatable time intervals, similar to major earthquakes on individual fault segments (Pagli et al., 2015). However, fewer constraints exist on whether nearby magmatic segments interact to potentially cause temporal clustering of rifting episodes on a broader scale (Ruch et al., 2021). In addition, and on a more fundamental level, quantitative constraints on the Holocene eruptive history of continental rift volcanoes are sparse, making quantification of the volcanic hazard prohibitively difficult (Wadge et al., 2016; Fontijn et al., 2018).

Here, we use new radiometric and geochemical constraints from the Boset, Kone and Fantale segments in the MER (Figure 1; Figure 2), to add detailed age constraints to previous absolute and relative chronological work (Wadge et al., 2016; Siegburg et al., 2018) and provide new evidence for a significant series of segment-scale rifting episodes between the late 18th to early 20th century CE. These data, in conjunction with other regional evidence, provide new age constraints of the most recent rift-wide episode of volcanism during magma-assisted rifting in the northern MER.

## 2 Geological background

Our study is in the MER, which currently extends at  $\sim 5 \text{ mm yr}^{-1}$  in a near E-W direction (Bendick et al., 2006; Birhanu et al., 2016) (Figure 1). Since the Quaternary, extension and volcanism in the MER has been mainly focused on a series of right stepping, en-echelon, magmatic segments including the Boset, Kone, and Fantale magmatic segments (Mohr, 1970; Ebinger and Casey, 2001; Kurz et al., 2007), which are part of the Wonji Fault Belt (WFB). These

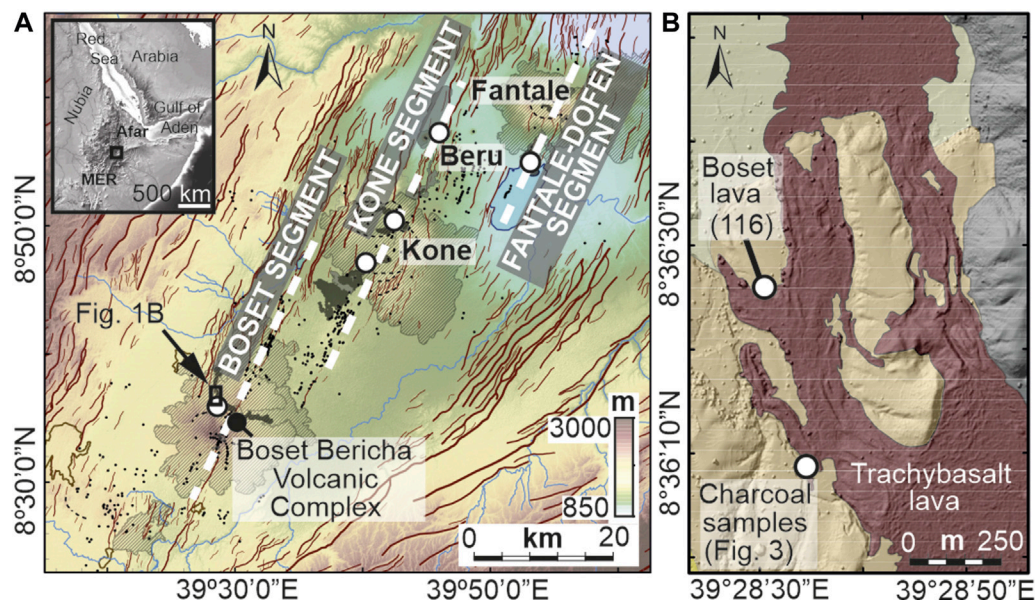
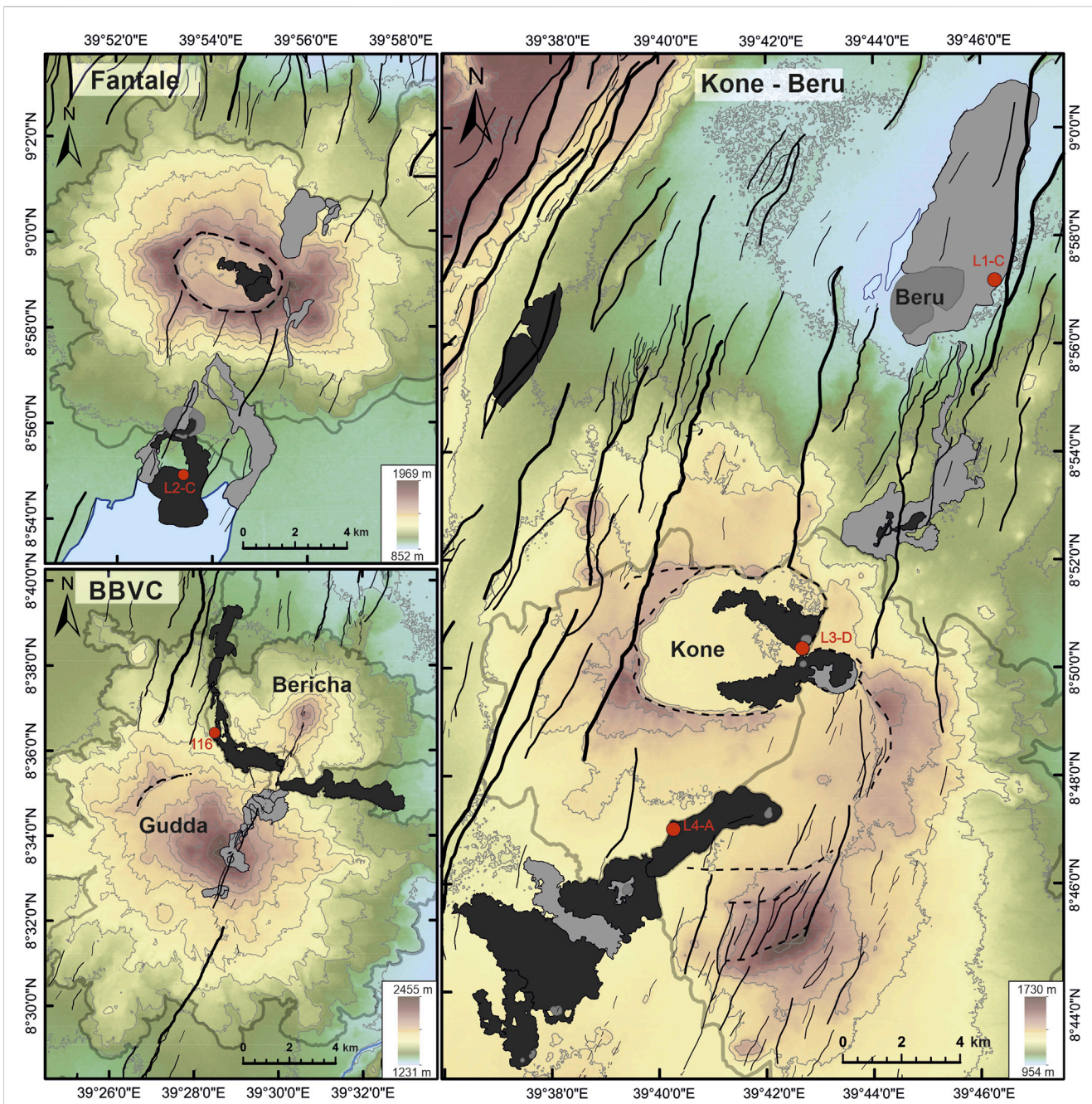


FIGURE 1

(A) Map of the northern Main Ethiopian Rift (MER). The inset shows the location of the study area (black box). The map shows the locations of the volcanoes (stippled pattern), and outlines of the studied lava flows (dark gray) from Boset, Kone and Fantale magmatic segments. Sample locations (white circles), scoria cones (black dots) and segments (white dashed lines; Kurz et al., 2007; Siegburg et al., 2020) are marked. Fault outlines (Siegburg et al., 2020) are marked in dark red lines. (B) The map of the young Boset lava flow, produced using LiDAR data (Keir et al., 2020), shows sampling locations of the Boset lava sample 116 and charcoal 114A, 114B (compare Figure 3). Beige and gray areas depict pre-existing lava flows (see Siegburg et al., 2018).



**FIGURE 2**  
 Maps of the spatial extent of the historical lava flows at (A) Fantale, (B) Kone, and (C) Boset magmatic segments. Maps are on top of a background of a shaded SRTM DEM with a resolution of 90 m, with black lines showing faults of the Wonji Fault Belt, dashed lines indicating the caldera outline (Siegburg et al., 2020), red dots showing sample location of this study and grey shaded areas illustrating the historical young flows.

segments are typically 40–70 km long, ~20 km wide and include the majority of the Holocene volcanic centers, monogenetic cone fields, and fissure swarms (Ebinger and Casey, 2001) (Figure 1). The magmatic segments are also the locus of modern day strain, with seismicity, geodetically detected volcano deformation and dike intrusion, and hydrothermal activity focused within them (Keir et al., 2006; Hunt et al., 2019; Temtime et al., 2020; Raggiunti et al., 2021; Albino et al., 2022).

Subsurface, wide-angle seismic reflection/refraction profiles (Mackenzie et al., 2005; Maguire et al., 2006) as well as

controlled source P-wave tomography (Keranen et al., 2004) image high P-wave velocities in the upper and mid crust beneath the magmatic segments. The seismic velocities, combined with collocated high densities constrained from gravity data are best modelled by mafic intrusions in the upper and middle crust beneath the segments (e.g., Cornwell et al., 2006; Nigussie et al., 2022). The subsurface evidence for localized mafic intrusion, combined with surface fissure swarms and cone fields, have previously been used to suggest that the localized extension across the segments is accommodated by episodic dike intrusion (Keir et al., 2006).

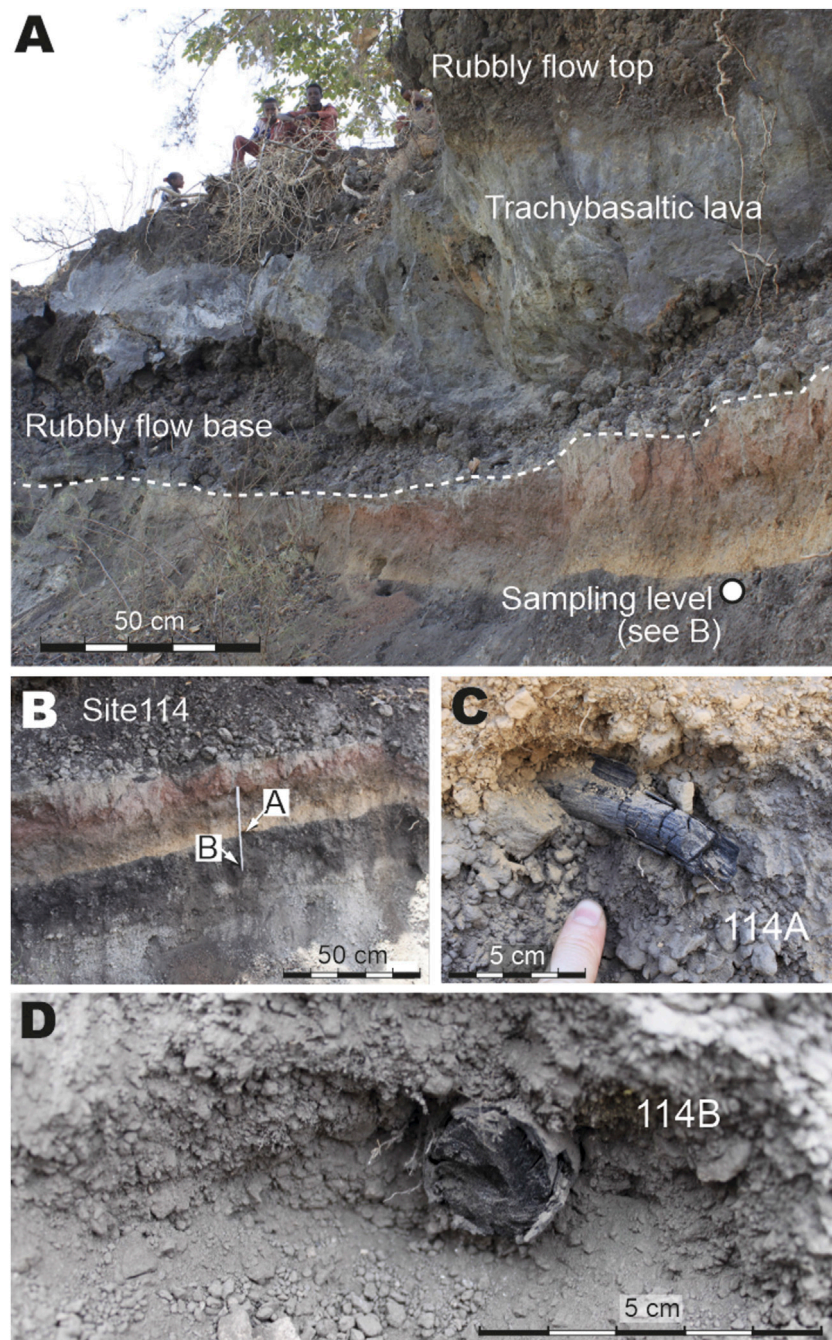


**FIGURE 3**

(A) Photograph of the base of the trachybasaltic lava flow at Boset-Bericha Volcanic Complex. (B) The image indicates the base of the flow and shows positions of charcoal fragments 114A and 114B. The photographs (C, D) show individual charcoal fragments 114A and 114B, respectively, recovered from a gray tephra layer underlying the lava.

The Boset-Bericha Volcanic Complex (BBVC) is in the middle of the Boset magmatic segment (Figure 1), and has a broad range of magmatic composition, and volcanic history typical of the magmatic centers within other Quaternary-Recent magmatic segments (Rooney et al., 2011). The Complex comprises the Gudda and Bericha centers which are built from flows which date from ~300 ka to the Holocene (Siegburg et al., 2018). These volcanic

deposits are mostly trachyte and peralkaline rhyolite lava flows, basaltic to intermediate fissures, and scoria cones (Siegburg et al., 2018). Several of the likely Holocene lavas are also associated with pyroclastic deposits (Fontijn et al., 2018). Evidence from local historical accounts, summarized from the original source in the results section (Harris, 1844), indicates that small-volume basaltic lavas were emitted at Kone and Fantale volcanoes during the early

1800s from fissures and cones aligned parallel to the rift (Williams et al., 2004; Wadge et al., 2016). Previous studies of these historical flows (e.g., Nicotra et al., 2021) have focused on their overall geochemical character and storage history in the crust. The flows were identified as Ti-rich aphyric basalts with geochemistry consistent with pre-eruptive storage in the lower crust (Nicotra et al., 2021).

### 3 Data and methods

For the radiocarbon dates, two charcoal fragments (114A, 114B) were recovered during fieldwork during April and May 2015 from a lapilli tuff underlying a ‘fresh’ mafic lava flow at the BBVC (Figures 2, 3; sample 116 and Phase P of Siegburg et al., 2018). The position of the studied lava flow was ~4 km to the west of Bericha, with mapping of the flow showing that it emanated from a NNE-SSW aligned central fissure linking Gudda and Bericha (Figures 1B, 2C). These samples were collected as representative samples for the described lava flow, based on sample location of historical accounts as well as vegetation and weathering state of the flows. The mapping of lava flows at Boset is based on Aster and LiDAR data (Keir et al., 2020) as well as field observation, described in Siegburg et al. (2018). The studied lava flows of the neighbouring segments are mapped using Google Earth satellite images and field observation. For Figures 1, 2 we also used SRTM data. The charcoal samples were radiocarbon dated at the Beta Analytic Laboratory (Miami, Florida, US) using acid/alkali/acid pretreatment procedures described at <http://www.radiocarbon.com>. Results were calibrated using the INTCAL13 database (Reimer et al., 2013) and OxCal v.4.2.4 (Bronk-Ramsey, 2013).

The historical constraints on eruption ages from the Kone and Fantale volcanoes were derived from the original historical document (Harris, 1844). The majority of more recent literature (e.g., Williams et al., 2004; Nicotra et al., 2021) commonly misconstrues the written records, and in particular place a far more precise date to the historical eruptions than are actually referred to in the original text. To address this, we quote in the results section key information from which a date range to these eruptions is assigned.

Major and trace element compositions were derived for a rock sample (116) from the recent lava flow at the Boset-Bericha Volcanic Complex that overlies the charcoal fragments (Figure 3), as well as from the fresh historical lava flows from the Kone and Fantale magmatic segments erupted from NNE striking fissures near the central volcanic edifices (Figure 2). More specifically, one sample was taken from the lava flow at Sabober cone just south of Fantale (Fantale, sample L2-C), two samples from different flows at Kone (Kone crater, sample L3-D) and just south of Kone (Kone south, sample L4-A), and then one sample from a fresh flow 20 km north of Kone (Beru, sample L1-C) (Figure 1; Figure 2). For the major elements, the four samples from Fantale, Kone, and Beru were analysed at University of Leicester, Department of Geology using PANalytical Axios Advanced XRF spectrometer, and the one sample from Boset-Bericha was measured using an Panalytical Magix-Pro WD-XRF fitted with a 4 kW Rh X-ray tube) at the University of Southampton. The trace element composition for all five samples were measured by ThermoScientific

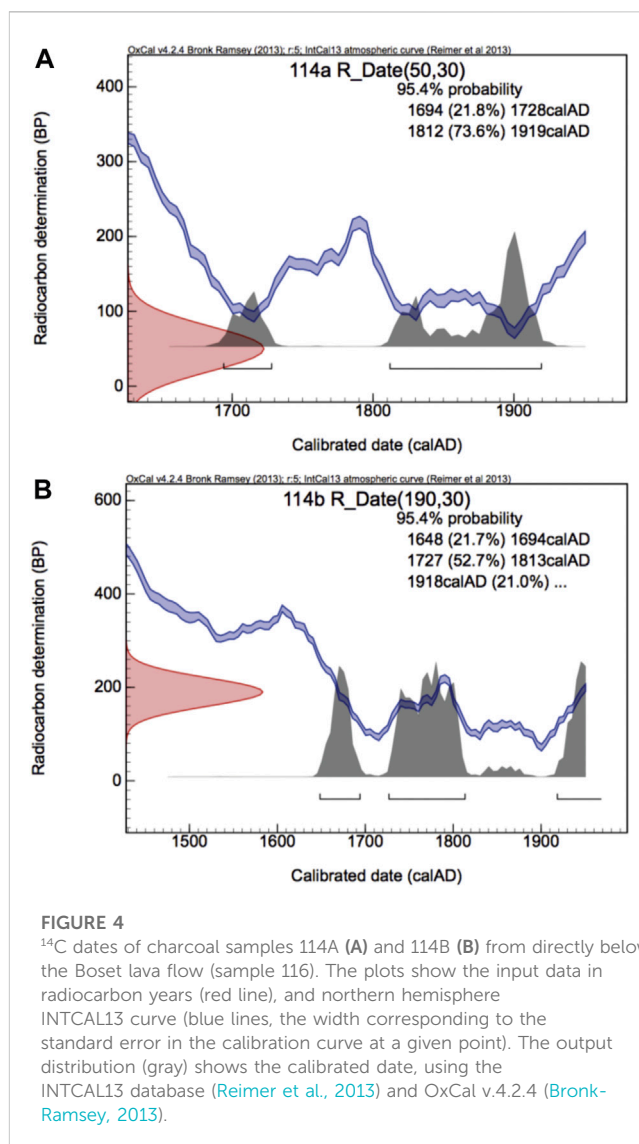


**FIGURE 4**  
<sup>14</sup>C dates of charcoal samples 114A (A) and 114B (B) from directly below the Boset lava flow (sample 116). The plots show the input data in radiocarbon years (red line), and northern hemisphere INTCAL13 curve (blue lines, the width corresponding to the standard error in the calibration curve at a given point). The output distribution (gray) shows the calibrated date, using the INTCAL13 database (Reimer et al., 2013) and OxCal v.4.2.4 (Bronk-Ramsey, 2013).

XSeries2 quadrupole inductively coupled plasma mass spectrometry (ICP-MS) at the University of Southampton.

## 4 Results

### 4.1 Radiometric ages

The retrieved radiocarbon dates from the two charcoal samples range from the 17th to the 20th century (Figure 4). Considering both samples individually at a 95% probability level, the peaks in likelihood for the formation of sample 114A is 1812 to 1919 calCE (73.6%) and 1694 to 1728 calCE (21.8%) (Figure 4). The <sup>14</sup>C dating for the sample 114B shows peaks in likelihood during 1727 to 1813 calCE (52.7%), 1648 to 1694 calCE (21.7%), and since 1918 calCE (21.0%). Since the highest likelihoods are 1812 to 1919 calCE for sample 114A and 1727 to 1813 calCE for 114B we further consider these individual ages.

**TABLE 1 Whole-rock composition of major (in wt%) and trace elements (in ppm), and mineral assemblage (in vol%) of young lava flows at Boset-Bericha Volcanic Complex (BBVC), Kone, Beru and Fantale volcanoes in the northern Main Ethiopian Rift.**

Volcano	BBVC		Kone		Beru	Fantale		
Sample	116 (a)	116 (b)	South L4-A	Crater L3-D	L1-C	L2-C(a)	L2-C(b)	L2-C(c)
SiO <sub>2</sub>	49.37		47.62	46.70	46.85	47.40		
TiO <sub>2</sub>	2.98		1.87	2.27	2.49	3.98		
Al <sub>2</sub> O <sub>3</sub>	14.51		14.31	14.98	15.40	13.72		
Fe <sub>2</sub> O <sub>3</sub> (tot)	13.72		11.77	12.66	13.35	15.68		
MnO	0.27		0.17	0.19	0.18	0.28		
MgO	4.04		11.06	8.81	7.94	4.79		
CaO	7.82		11.01	10.74	10.63	9.20		
Na <sub>2</sub> O	4.47		2.54	3.19	2.96	3.98		
K <sub>2</sub> O	1.12		0.63	1.08	0.70	0.92		
P <sub>2</sub> O <sub>5</sub>	1.03		0.35	0.55	0.46	1.16		
SO <sub>3</sub>	-		0.01	0.01	0.06	0.08		
LOI	-0.40		-0.49	-0.47	-0.41	-0.72		
Total	98.93		100.85	100.71	100.61	100.49		
Li	6.92	9.16	4.53	5.78	4.81	5.95	5.71	5.74
Sc	30.26	41.35	31.87	29.09	30.57	32.73	33.83	33.40
Ti	17,710	18,330	10,570	12,810	14,000	22,710	24,110	24,010
V	210.50	236.20	266.80	268.20	295.40	287.50	294.40	306.00
Cr	3.24	8.81	658.20	346.90	190.20	1.47	0.61	0.85
Co	24.64	27.42	50.71	47.24	46.68	33.11	33.34	34.88
Ni	7.42	9.42	188.20	124.10	52.52	1.48	1.13	1.26
Cu	33.81	35.69	71.49	69.38	55.79	13.56	14.91	14.45
Rb	22.27	26.18	12.06	26.79	12.24	17.22	17.68	16.20
Sr	456.90	512.20	365.50	562.20	459.90	462.50	474.40	477.00
Y	38.56	39.56	21.01	24.89	22.77	39.66	42.54	41.88
Zr	171.00	179.20	110.90	158.50	134.90	161.20	160.40	164.50
Nb	32.68	33.54	19.81	37.69	21.85	31.36	32.45	33.79
Sn	1.34		0.83	1.08	1.01	1.20	1.20	
Cs	0.24	0.37	0.12	0.32	0.12	0.17	0.18	0.16
Ba	622.5	605.0	231.1	389.8	278.0	489.3	498.6	503.6
La	31.50	32.35	16.58	30.04	19.17	30.35	30.74	31.48
Ce	72.61	73.98	36.38	61.99	42.37	70.68	71.13	72.61
Pr	9.77	9.65	4.73	7.48	5.56	9.44	9.58	9.68
Nd	43.11	42.15	19.94	29.79	23.54	42.08	43.29	43.60
Sm	9.49	9.20	4.50	6.07	5.24	9.50	9.78	9.91
Eu	3.84	3.58	1.56	2.06	1.88	3.69	3.66	3.81
Gd	9.35	9.14	4.45	5.68	5.15	9.55	9.75	10.06
Tb	1.33	1.30	0.68	0.83	0.76	1.35	1.41	1.41

(Continued on following page)

**TABLE 1 (Continued)** Whole-rock composition of major (in wt%) and trace elements (in ppm), and mineral assemblage (in vol%) of young lava flows at Boset-Bericha Volcanic Complex (BBVC), Kone, Beru and Fantale volcanoes in the northern Main Ethiopian Rift.

Volcano	BBVC		Kone		Beru	Fantale		
Sample	116 (a)	116 (b)	South L4-A	Crater L3-D	L1-C	L2-C(a)	L2-C(b)	L2-C(c)
Dy	7.39	7.25	3.92	4.71	4.36	7.57	7.82	7.83
Ho	1.42	1.38	0.77	0.91	0.85	1.44	1.51	1.49
Er	3.64	3.59	2.06	2.40	2.23	3.73	3.87	3.87
Tm	0.50	0.48	0.29	0.33	0.31	0.50	0.52	0.52
Yb	3.07	3.01	1.84	2.09	1.89	3.05	3.17	3.20
Lu	0.45	0.44	0.27	0.31	0.28	0.44	0.47	0.47
Hf	4.17	4.14	2.58	3.49	3.09	3.72	3.84	3.88
Ta	2.44	2.27	1.35	2.25	1.38	2.15	2.34	2.35
Pb	3.44	3.12	1.82	2.71	2.08	1.93	1.96	1.79
Th	2.66	2.78	1.45	3.00	1.48	2.19	2.25	2.22
U	0.71	0.68	0.38	0.77	0.40	0.59	0.62	0.59
Zn		116.60						133.70
Ol	3		15			4		
Cpx	5		15			6		
Plag	20		7		40	40		
Opaques	2				2	20		
Groundmass	60		43					
Vesicles	10		10–20		10–15	30		

## 4.2 Historical records

The dates of the most recent fissural eruptions from Fantale and Kone are constrained from historical records. The following account from [Harris \(1844\)](#) on page 301 refers to the crater of Saboo (i.e., Sabober) and Sahela Selassie's grandsire (grandfather) that is Asfaw Wossen (ruler of Shewa), who reigned between c. 1770 and c. 1808:

“In an easterly direction the course was bounded by the great isolated crater of Saboo, yawning in the very centre of a well populated plain, and said to have been in full activity in the time of Sahela Selassie's grandsire, who reigned only 30 years ago; an assertion which was fully borne out by the recent appearance of the lava streams. The long-horned oryx, with great herds of antelope, grazed around every pool—the latter little disturbed by the presence of those who tended the flocks of sheep and goats, and whose groups of circular wigwams peeped forth in every sequestered corner.”

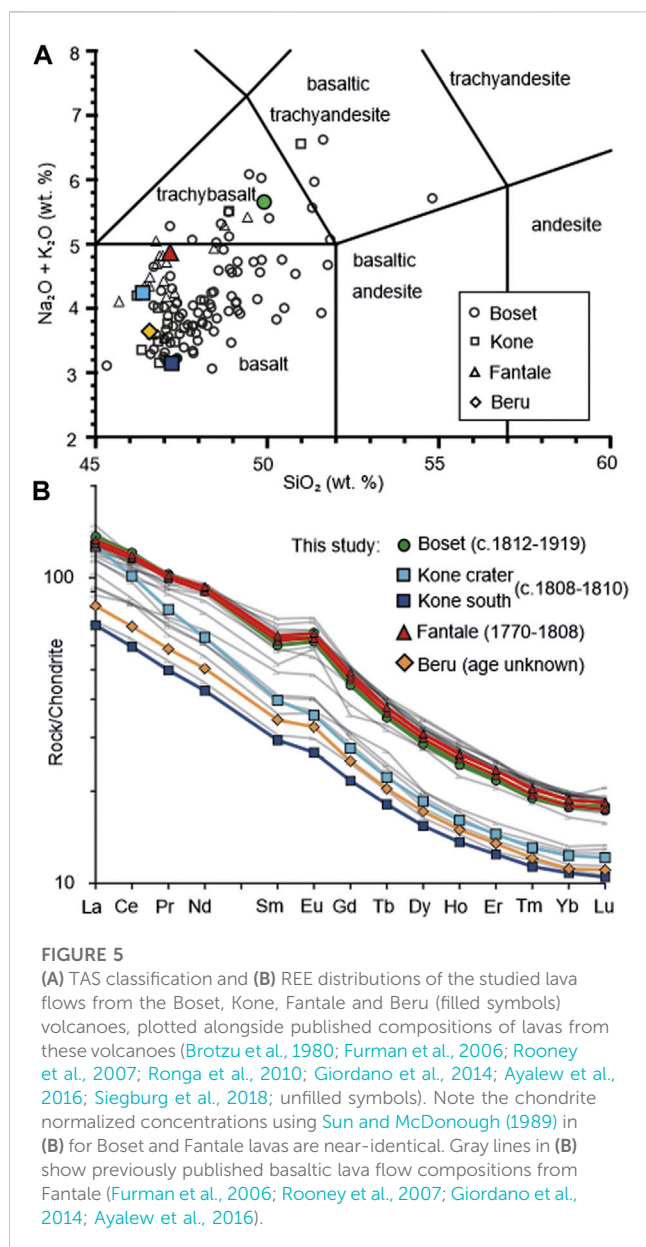
Fantale is commonly referred in literature to have erupted between 1810 and 1820 CE ([Williams et al., 2004](#); [Nicotra et al., 2021](#)). However, [Harris \(1844\)](#) cites local reports that the eruption occurred during the reign of Asfaw Wossen, i.e., between approximately 1770 and 1808 CE.

[Harris \(1844\)](#) page 302 also refers to the crater of Winzegeor, currently known as Kone crater ([Williams, 2016](#)), or previously known as Gariboldi ([Cole, 1969](#)). In this text an approximate

eruption age of 1810 CE for the Kone crater is made: “The next object was to visit the far-famed volcanic well of Boorchutta, on the frontier of Mentshar, bordering on the wilderness of Taboo, which was to limit the wanderings of the party. Shortly after gaining the summit of the Kozi mountain, the road wound along the very brink of the gaping crater of Winzegeor, from whose monstrous chasm the entire adjacent country has been recently overflowed. Extending two miles in length by one and a half in breadth, it is environed by perpendicular walls towering from six to eight hundred feet, two gorges to the east and southeast having afforded an outlet to the boiling deluge. The area of the whole basin affords occasional glimpses of jet black through belts of the most brilliant verdure; and two bare truncated cones, thrown up during an eruption some 30 years previously, having poured a serpentine stream high over the surrounding jungles, remain dark and cindery as on the day when they were vomited by the pillared flame from the bowels of the great abyss”.

## 4.3 Petrography and geochemistry of Boset, Kone, and Fantale lavas

The selected lavas are phaneritic to porphyritic in texture, consisting of 3–5 vol% olivine, 5 vol% clinopyroxene, 7–40 vol% plagioclase, 1–20 vol% opaque phenocrysts and 10–30 vol% vesicles.



Petrographically, the rocks are distinct from each other with a larger proportion of olivine and clinopyroxene (up to 15 vol%) within the two Kone samples, and Fantale and Beru lavas typically exhibiting a smaller crystal size. The groundmass of the Boset lava flow sample have mingling textures.

Based on the total-alkali-silica (TAS) diagram (Le Bas et al., 1986), the Boset lava (sample 116), that overlies the charcoal at Boset (Figure 3), is a trachy-basalt whilst the Fantale and Kone lavas are basaltic in composition (Table 1; Figure 5). The total-alkali value ( $K_2O + Na_2O$ ) for all lavas range between 3.1 and 5.7 wt% with corresponding  $SiO_2$  values of 46.4 to 49.9 wt% (Figure 5). All samples display a narrow range of concentrations for  $SiO_2$ ;  $Al_2O_3$  (13.7–15.4 wt%);  $Fe_2O_3$  (12.7–15.7 wt%) and  $MnO$  (0.2–0.3 wt%) yet a larger range for  $MgO$  (4.1–11.0 wt%),  $TiO_2$  (1.9–4.0 wt%);  $P_2O_5$  (0.35–1.16 wt%),  $CaO$  (7.8–11.0 wt%),  $Na_2O$  (2.5–4.5 wt%),  $K_2O$  (0.6–1.1 wt%) (Table 1). The Boset lava (sample 116) is

distinctive from the volcanic products of the neighbouring edifices by its higher  $SiO_2$  value (49.9 wt%), combined with a lower  $MgO$  (4.1 wt%) and  $CaO$  (7.9 wt%). The Boset lava also exhibits a lower  $CaO/Al_2O_3$  ratio (0.54) compared to that of Fantale (0.67), Beru (0.69) and Kone (0.72–0.77), further demonstrating the more evolved composition of the Boset lava (sample 116) (Siegburg et al., 2018).

Zr concentrations range from 111 to 179 ppm, with the trachybasalt of Boset having the highest Zr concentration (179 ppm, Table 1). The Y concentrations of Kone volcanics range from 21 to 25 ppm yet the Boset and Fantale volcanics have higher Y concentrations (39.7–42.5 ppm and 38.6–39.6 ppm, respectively, Table 1). A similar trend is observed in Nd for Kone (incl. Beru) lavas having concentrations of 19.9 to 29.8 ppm, but Nd of Boset and Fantale are ranging between 42.1 and 43.6 ppm (Table 1). Ba and Pb are the only trace elements where the concentrations are substantially different at Boset (605–623 ppm and 3.1–3.4 ppm, respectively), Kone (231–390 ppm and 1.8–2.7 ppm, respectively) and Fantale (489–504 ppm and 1.8–2.0 ppm, respectively, Table 1). Further differences among the lava flows are within the trace metals Cr, Ni and Cu, where concentration is most enriched in Kone lavas, less enriched in Boset lavas, and lowest in lavas of the Fantale segment (Table 1).

Chondrite-normalized rare earth element (REE) patterns are sub-parallel for all lavas (except Kone crater lava flow), exhibiting a marked enrichment in light-REE (LREE;  $La_n/Sm_n$  2.0–2.3), and a mild enrichment in the middle-REE (MREE) relative to the heavy-REE (HREE;  $Dy_n/Yb_n$  1.4–1.6) (Figure 5). The Kone crater lava flow can be distinguished by its steeper LREE profile ( $La_n/Sm_n$  3.1) compared to the other lavas (Figure 5). The lavas from Boset and Fantale are almost indistinguishable in terms of their chondrite normalised REE concentrations (Figure 5). Primitive-mantle-normalised trace element profiles reveal a negative Pb anomaly within the Fantale lavas not observed within the Boset lava (Figure 5).

## 5 Discussion

Our radiometric  $^{14}C$  age constraint of *in situ* charcoal found below the youngest mafic lava flow of the Boset-Bericha Volcanic Complex (Siegburg et al., 2018) allows us to infer the age of the most recent mafic volcanic activity. When considered the  $^{14}C$  age probability distribution between the two charcoal samples individually, the two charcoal sample locations are proximal to one another (Figure 3) with only 50–100 years difference in age (Figure 4). This scenario would be possible within a single tree trunk by considering, for example, the “old wood effect” (Bowman, 1990). If the samples are from neighbouring trees, the lava flow age would more likely represent the youngest of the two samples and therefore 1812 to 1919 CE. We therefore favour the interpretation of the Boset lava flow age as 1812 to 1919 CE.

In the context of other chronological stratigraphic, and regional historic constraints, our  $^{14}C$  age constraint of Boset charcoal is a detailed addition to the previous age estimation of  $13 \pm 8.3$  ka for the overlying lava flow, analysed in three runs by  $^{40}Ar/^{39}Ar$  dating (Siegburg et al., 2018). The uncertainty of two of the aliquots of the  $^{40}Ar/^{39}Ar$  dates are consistent with the  $^{14}C$  constraints.

Differences between both age constraints are due to the different resolution of the methods for young samples as well as the lower potassium content in the groundmass and possibly by contamination due to the presence of mingling textures for the sample used in  $^{40}\text{Ar}/^{39}\text{Ar}$  dating (Siegburg et al., 2018).

The thickness of the soil horizon overlying lavas and tuffs (Figure 3) in the vicinity provides an additional constraint because soils generally accumulate at a given rate depending on their geographic location (e.g., Bunting, 2020). The andosol (i.e., a soil containing volcanic tephra) is typically 20–25 cm thick, with no evidence for reworking (Figure 3). Soil formation rates in the Shewa region of Ethiopia at this elevation (c. 1,630 m above sea-level) are on the order of 10 t/ha/yr (Hurni, 1983). Assuming a typical andosol density of 900 kg/m<sup>3</sup> (Batjes and Dijkshoorn, 1999), this gives an accumulation rate of ~0.1 cm per year. As such, observed soil thicknesses are commensurate with eruptive activity last occurring at around 1765 to 1815 CE. The combined  $^{14}\text{C}$  age range, 1812 to 1919 CE, is broadly consistent with this. This would make the youngest mafic Boset eruption roughly contemporaneous with similar lava flows from Kone volcano and the Sabober crater at Fantale (Figure 1; Figure 2), suggested by historic records (Harris, 1844).

Mapping these lava flows of Boset, Kone, Beru and Fantale by remote sensing data, they have a similar appearance in colour and freshness. This may suggest similar composition (Figure 5), similar vegetation and weathering state, similar roughness and texture (AA lava) of the surface and/or similar eruption age. The similarity of the surface texture and vegetation and weathering state is ground-truthed by field observation during sampling for Kone, Fantale and Boset lava flows. The lava flow at Beru on the northern part of the Kone segment is mafic in composition, with the flow surface in the field being slightly more vegetated and weathered as well as more smoothed and less blocky. The absolute age of Beru lava flow is not dated yet, however we interpret the volcanic activity of Beru to be possible within a similar time frame as the other studied historical lava flows. The different surface appearance of Beru lava flow can be due to secondary processes such as seasonal variation and by water accumulation due to the lower topography and normal fault offsets (Figure 2) or due to slightly earlier eruption age.

Our  $^{14}\text{C}$  dates and other age constraints in the Boset, Kone, and Fantale segments, suggest that as a conservative estimate all three rifting episodes occurred within about 2–3 centuries of each other, between 1648 and 1919 CE, but most likely within a narrower time window within the late 18th to early 20th centuries. The lavas were erupted from fissures aligned along major faults in their respective segments (Williams et al., 2004; Kurz et al., 2007; Siegburg et al., 2018). This process is thought to repeatedly occur in individual segments every 100–400 years (Pagli et al., 2015; Siegburg et al., 2018) when considering a dyke width of 0.5–2 m and rift extension rates of 5 mm/year (Bendick et al., 2006). Furthermore, 50 km south of the BBVC, a comenditic fissure system (Giano domes) at Tullu Moye volcano is thought to have been active during 1900 CE (Gouin, 1979; Wooley, 2001; Fontijn et al., 2018). Therefore, the recent eruption from the BBVC could be part of a more extensive period of unrest along the very northern part of the East African rift (see Wadge et al., 2016).

Given that the suite of fissure eruptions from Boset, Fantale, and Kone occur within time windows that potentially overlap, we

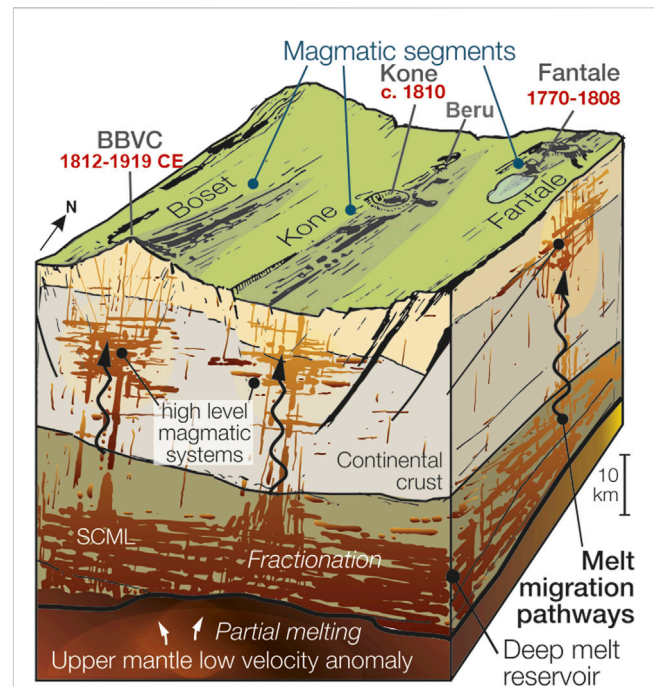


**FIGURE 6**

Cartoon showing the inferred structure and magmatic systems of three segments of the Ethiopian rift. Magmas episodically rise from the mantle melt region to a deep lithospheric melt reservoir, where fractionation occurs. These juvenile mafic melts are then supplied to sub-volcanic plumbing systems in discrete segments, where they are modified through interaction with crust and sediments. SCML = sub-continental mantle lithosphere, BBVC = Boset-Bericha Volcanic Complex.

use the geochemical data to test whether these eruptions are likely related to a single, multi-segment long dike intrusion, or to individual shorter dikes beneath each discrete segment. All studied lavas fall within the broad chemical range previously observed at these volcanoes (Figure 5), (e.g., Furman et al., 2006; Peccerillo et al., 2007; Rooney et al., 2007; Ronga et al., 2010; Giordano et al., 2014; Ayalew et al., 2016; Siegburg et al., 2018; Nicotra et al., 2021). However, they do differ in their petrography and geochemistry, suggesting variations in mineral proportions and/or composition alongside difference in the degree of fractionation between mafic magmas (basalt to trachy-basalt) of neighbouring segments (Figure 5; Table 1). In the Kone lava flows, which contain a larger proportion of olivine and clinopyroxene, the higher MgO, Fe<sub>2</sub>O<sub>3</sub>, MnO, and TiO<sub>2</sub> together with high Ni and Cr, and low Zr suggest a more primitive composition compared to the neighbouring magmatic segments. The lava of Beru is geochemically most similar to the lava of Kone south, consistent with their shared location of the same segment. Both exhibit similar REE trends, with the lower REE concentrations for the Kone south lava most likely due to a lower degree of fractionation (Figure 5). Higher values of Nb/Yb, Th/La, La/Sm, relative enriched LREE patterns and slightly enriched alkali content for the lava flow at Kone crater suggest a lower degree of parental partial melting and/or deeper source compared to the other samples of Kone and other segments. These geochemical differences imply variation in mineral composition, source

heterogeneity, degree of partial melting (e.g., Rooney et al., 2007) or different ascent and pre-eruptive storage dynamics (Nicotra et al., 2021) within a tectono-magmatic segment.

The recent Boset and Fantale lavas differ geochemically from those at Kone but are near-identical in terms of their REE distributions (Figure 5B), again suggesting a similar degree of fractionation. The Fantale lava differs from the Boset lava only in terms of its higher  $\Delta\text{Nb}$  value (defined by Fitton et al., 1997) of 0.47–0.52 (Fantale) and 0.40–0.42 (Boset), and Ce/Pb of >36 (Fantale) and 21.1–23.7 (Boset), which is consistent with other samples of Fantale (Rooney et al., 2007) possibly indicating heterogeneous mantle and plume composition (e.g., Fitton et al., 1997) or that local shallow processes occur only in the Fantale segment. Sulphur saturation and segregation (Mavrogenes and O'Neill, 1999) during magma evolution would decrease Pb (flow out by fluids) and therefore increase Ce/Pb ratios. This is consistent with low Ni and Cu values within the samples (Table 1). These geochemical variations between and within segments cannot be explained only by fractional crystallisation. We also interpret that a heterogeneous mantle composition (e.g., Daoud et al., 2010) as well as shallow crustal processes (e.g., Rooney et al., 2007) may contribute to the geochemical differences observed. Overall, the geochemical variability strongly points towards the fissural eruptions at the three magmatic segments each being fed by a discrete intrusion, which favours an interpretation of rifting episodes within discrete magmatic segments but with these discrete episodes being somewhat clustered in time (Figure 6).

Our favoured interpretation is supported by the distance (~60-km) between each eruptive fissure and en-echelon arrangement of the magmatic segments (Figure 1). While a >100 km lateral magma transport is not uncommon in the geological record (e.g., Isle of Mull, Ishizuka et al., 2017), there are no modern-day documented examples of diking events that transect multiple segments within an intracontinental rift. Instead, both observations and models point towards single segment-scale rifting episodes potentially being clustered in time. For example, further north of the MER in the Afar depression, southern Red Sea and western Gulf of Aden, Ruch et al. (2021) identify a clear regional increase in earthquake swarms and volcanic eruptions within discrete magmatic segments during the period from ~2003 to 2013. The clustered timing of these multiple segment scale rifting episodes was interpreted as potentially driven from the magma source, with a pulse of melt input into a shared deep crustal or upper mantle reservoir (Ruch et al., 2021). Alternatively, the temporal clustering could be explained by dike induced stress changes from each rifting episode causing a positive Coulomb stress change in the neighbouring segment, aiding the triggering of a temporally linked series of rifting events (Ayele et al., 2007; Ruch et al., 2021). Both hypotheses can explain the Fantale, Kone and Boset rifting episodes.

## 6 Conclusion

In summary, we conduct new radiocarbon dating from a recent lava flow at the Boset magmatic segment of the Ethiopian rift, and combine this with historical dating of similarly historical lava flows in the adjacent magmatic segments. New radiocarbon

dates of multiple charcoal samples from the base of the most recent fissural lava at Boset indicate that it likely occurred between 1812 and 1919 CE, a date range that is similar to those from historical accounts of fissural eruptions from the neighbouring Kone (~1810 CE) and Fantale (~1770 to 1808 CE) magmatic segments. New analysis of major elements compositions from these historical fissural lavas from all three magmatic segments show compositions that vary in the basalt and trachybasalt fields, with sufficient variation to rule out them having erupted from a single dike intrusion. This, combined with the scatter in dates from the radiocarbon analysis and historical accounts, along with the location of each eruption in a discrete and spatially offset magmatic segment, favours an interpretation that each magmatic segment ruptured during a discrete rifting episode, but that these were clustered in time across multiple segments of the rift. Mechanisms to explain the clustering are more speculative but could include stress transfer from dike intrusion and deep crustal hydraulic connection in the plumbing system of multiple segments.

## Data availability statement

The original contributions presented in the study are included in the article, further inquiries can be directed to the corresponding author.

## Author contributions

MS, TMG, DK and JMB contributed to the conception and design of the study and performed the fieldwork, analyses, and writing of the manuscript. TG helped collecting the lava flow samples. EFG contributed to the fieldwork in Ethiopia. RNT and EJW helped with analyses and discussion of the geochemical results.

## Funding

Gernon is supported by the Natural Environment Research Council, NERC (grant NE/R004978/1) and DK, Greenfield and MS were supported by the NERC RiftVolc project (grant NE/L013509/1). EJW is supported by NERC Spitfire studentship grant NE/L002531/1. We used LiDAR data collected by the NERC Airborne Research and Survey Facility (ARSF), grant ET12-14.

## Acknowledgments

We thank the RiftVolc community for thoughtful interactions over many meetings. We thank staff of the Institute of Geophysics, Space Science and Astronomy and Department of Earth Science at Addis Ababa University, Ethiopia for support during fieldwork. Radiocarbon dating was performed by the Beta Analytic Laboratory (Florida, US). We acknowledge skillful analytical assistance from Andy Milton, Matthew Cooper and Agnes Michalik (University of Southampton) and Tom Knott (University of Leicester). We would like to thank the reviewers Francesco Mazzarini and Gabriel Ureta

and the editor Karoly Nemeth for their constructive comments that improve the manuscript.

## Conflict of interest

The authors declare that the research was conducted in the absence of any commercial or financial relationships that could be construed as a potential conflict of interest.

## References

- Albino, F., Biggs, J., Lazecký, M., and Maghsoudi, Y. (2022). Routine processing and automatic detection of volcanic ground deformation using sentinel-1 InSAR data: Insights from african volcanoes. *Remote Sens.* 14, 5703. doi:10.3390/rs14225703
- Ayalew, D., Jung, S., Romer, R. L., Kersten, F., Pfänder, J. A., and Garbe-Schönberg, D. (2016). Petrogenesis and origin of modern Ethiopian rift basalts: Constraints from isotope and trace element geochemistry. *Lithos* 258 (259), 1–14. doi:10.1016/j.lithos.2016.04.001
- Ayele, A., Jacques, E., Kassim, M., Kidane, T., Omar, A., Tait, S., et al. (2007). The volcano–seismic crisis in Afar, Ethiopia, starting September 2005. *Earth Planet. Sci. Lett.* 255, 177–187. doi:10.1016/j.epsl.2006.12.014
- Barnie, T. D., Keir, D., Hamling, I., Hofmann, B., Belachew, M., Carn, S., et al. (2016). A multidisciplinary study of the final episode of the Manda Hararo dyke sequence, Ethiopia, and implications for trends in volcanism during the rifting cycle. *Geol. Soc. Lond. Spec. Publ.* 420, 149–163. doi:10.1144/SP420.6
- Batjes, N. H., and Dijkshoorn, J. A. (1999). Carbon and nitrogen stocks in the soils of the Amazon Region. *Geoderma* 89, 273–286. doi:10.1016/S0016-7061(98)00086-X
- Bendick, R., McClusky, S., Bilham, R., Asfaw, L., and Klemperer, S. (2006). Distributed Nubia–Somalia relative motion and dike intrusion in the Main Ethiopian Rift. *Geophys. J. Int.* 165, 303–310. doi:10.1111/j.1365-246X.2006.02904.x
- Birhanu, Y., Bendick, R., Fisseha, S., Lewi, E., Floyd, M., King, R., et al. (2016). GPS constraints on broad scale extension in the Ethiopian Highlands and Main Ethiopian Rift. *Geophys. Res. Lett.* 43, 6844–6851. doi:10.1002/2016GL069890
- Bowman, S. (1990). *Radiocarbon dating - Interpreting the past*. Berkeley: Univ of California Press.
- Bronk-Ramsey, C. (2013). Bayesian analysis of radiocarbon dates. *Radiocarbon* 51, 337–360. doi:10.1017/s0033822200033865
- Brotzu, P., Morbidelli, L., Piccirillo, E. M., and Traversa, G. (1980). Volcanological and magmatological evidence of the boseti volcanic complex (Main Ethiopian rift). *Atti Convegno Lincei* 47, 317–366.
- Bunting, B. T. (2020). *The geography of soil*. Routledge library Editions: Geology, Band, 1–216.
- Carbotte, S. M., Smith, D. K., Cannat, M., and Klein, E. M. (2016). Tectonic and magmatic segmentation of the global ocean ridge system: A synthesis of observations. *Geol. Soc. Lond. Spec. Publ.* 420, 249–295. doi:10.1144/SP420.5
- Cole, J. W. (1969). Gariboldi volcanic complex, Ethiopia. *Bull. Volcanol.* 33, 566–578. doi:10.1007/bf02596525
- Cornwell, D. G., Mackenzie, G. D., England, R. W., Maguire, P. K. H., Asfaw, L. M., and Oluma, B. (2006). Northern Main Ethiopian Rift crustal structure from new high-precision gravity data. *Geol. Soc. Lond. Spec. Publ.* 259, 307–321. doi:10.1144/GSL.SP.2006.259.01.23
- Daoud, M. A., Maury, R. C., Barrat, J.-A., Taylor, R. N., Le Gall, B., Guillou, H., et al. (2010). A LREE-depleted component in the Afar plume: Further evidence from Quaternary Djibouti basalts. *Lithos* 114 (3–4), 327–336. doi:10.1016/j.lithos.2009.09.008
- Ebinger, C. J., and Casey, M. (2001). Continental breakup in magmatic provinces: An Ethiopian example. *Geology* 29, 527–530. doi:10.1130/0091-7613(2001)029<0527:CBIMPA>2.0.CO;2
- Fitton, J. G., Saunders, A. D., Norry, M. J., Hardarson, B. S., and Taylor, R. N. (1997). Thermal and chemical structure of the Iceland plume. *Earth Planet. Sci. Lett.* 153 (3–4), 197–208. doi:10.1016/S0012-821X(97)00170-2
- Fontijn, K., McNamara, K., Zafu Tadesse, A., Pyle, D. M., Dessalegn, F., Hutchison, W., et al. (2018). Contrasting styles of post-caldera volcanism along the Main Ethiopian Rift: Implications for contemporary volcanic hazards. *J. Volcanol. Geotherm. Res.* 356, 90–113. doi:10.1016/j.jvolgeores.2018.02.001
- Furman, T., Bryce, J., Rooney, T., Hanan, B., Yirgu, G., and Ayalew, D. (2006). Heads and tails: 30 million years of the Afar plume. *Geol. Soc. Spec. Publ.* 259, 95–120. doi:10.1144/GSL.SP.2006.259.01.09
- Giordano, F., D’Antonio, M., Civetta, L., Tonarini, S., Orsi, G., Ayalew, D., et al. (2014). Genesis and evolution of mafic and felsic magmas at quaternary volcanoes within the Main Ethiopian Rift: Insights from Fedemsa and Fanta’Ale complexes. *Lithos* 188, 130–144. doi:10.1016/j.lithos.2013.08.008
- Gouin, P. (1979). *Earthquake history of Ethiopia and the horn of africa*. Ottawa, Ontario: International Development Research Centre IDRC.
- Harris, W. C. (1844). *Highlands of Ethiopia*. New York: J. Winchester, New World Press.
- Hayward, N. J., and Ebinger, C. J. (1996). Variations in the along-axis segmentation of the Afar Rift system. *Tectonics* 15, 244–257. doi:10.1029/95TC02292
- Hunt, J. A., Pyle, D. M., and Mather, T. A. (2019). The geomorphology, structure, and lava flow dynamics of peralkaline rift volcanoes from high-resolution digital elevation models. *Geochem. Geophys. Geosystems* 20, 1508–1538. doi:10.1029/2018GC008085
- Hurni, H. (1983). “Ethiopian Highlands reclamation study: Soil formation rates in Ethiopia,” in *Land use planning and regulatory department* (United Nations: Ministry of Agriculture, Food and Agriculture Organization).
- Ishizuka, O., Taylor, R. N., Geshi, N., and Mochizuki, N. (2017). Large-volume lateral magma transport from the Mull volcano: An insight to magma chamber processes. *Geochem. Geophys. Geosystems* 18, 1618–1640. doi:10.1002/2016GC006712
- Keir, D., Bull, J., Gernon, T., Siegburg, M., and Ayele, A. (2020). *LiDAR DEM of Boset volcano in Ethiopia*. University of Southampton. doi:10.5258/SOTON/D1347
- Keir, D., Ebinger, C. J., Stuart, G. W., Daly, E., and Ayele, A. (2006). Strain accommodation by magmatism and faulting as rifting proceeds to breakup: Seismicity of the northern Ethiopian rift. *J. Geophys. Res.* 111, B5. doi:10.1029/2005JB003748
- Keranen, K., Klemperer, S., and Gloaguen, R. (2004). Three-dimensional seismic imaging of a protoridge axis in the Main Ethiopian Rift. *Geology* 32, 949–952. doi:10.1130/G20737.1
- Kurz, T., Gloaguen, R., Ebinger, C., Casey, M., and Abebe, B. (2007). Deformation distribution and type in the Main Ethiopian rift (MER): A remote sensing study. *J. Afr. Earth Sci.* 48, 100–114. doi:10.1016/j.jafrearsci.2006.10.008
- Le Bas, M. J., Le Maitre, R. W., Streckeisen, A., and Zanettin, B. (1986). A chemical classification of volcanic rocks based on the total alkali-silica diagram. *J. Petrol.* 27, 745–750. doi:10.1093/petrology/27.3.745
- Mackenzie, G. D., Thybo, H., and Maguire, P. K. H. (2005). Crustal velocity structure across the Main Ethiopian rift: Results from two-dimensional wide-angle seismic modelling. *Geophys. J. Int.* 162, 994–1006. doi:10.1111/j.1365-246X.2005.02710.x
- Maguire, P. K. H., Keller, G. R., Klemperer, S. L., Mackenzie, G. D., Keranen, K., Harder, S., et al. (2006). Crustal structure of the northern Main Ethiopian Rift from the EAGLE controlled-source survey; a snapshot of incipient lithospheric break-up. *Geol. Soc. Lond. Spec. Publ.* 259, 269–292. doi:10.1144/gsl.sp.2006.259.01.21
- Mavrogenes, J. A., and O’Neill, H. St.C. (1999). The relative effects of pressure, temperature and oxygen fugacity on the solubility of sulfide in mafic magmas. *Geochimica Cosmochimica Acta* 63 (7/8), 1173–1180. doi:10.1016/S0016-7037(98)00289-0
- Mohr, P. A. (1970). Volcanic composition in relation to tectonics in the Ethiopian Rift System: A preliminary investigation. *Bull. Volcanol.* 34, 141–157. doi:10.1007/bf02597782
- Nicotra, E., Viccaro, M., Donato, P., Acocella, V., and De Rosa, R. (2021). Catching the Main Ethiopian Rift evolving towards plate divergence. *Sci. Rep.* 11, 21821. doi:10.1038/s41598-021-01259-6
- Nigussie, W., Mickus, K., Keir, D., Alemu, A., Muhabaw, Y., Muluneh, A. A., et al. (2022). Subsurface structure of magmatic segments during continental breakup: Perspectives from a gravity data analysis along the Main Ethiopian Rift. *Front. Earth Sci.* 10, 2759. doi:10.3389/feart.2022.1092759
- Pagli, C., Mazzarini, F., Keir, D., Rivalta, E., and Rooney, T. O. (2015). Introduction: Anatomy of rifting: Tectonics and magmatism in continental rifts, oceanic spreading centers, and transforms. *Geosphere* 11, 1256–1261. doi:10.1130/GES01082.1

## Publisher’s note

All claims expressed in this article are solely those of the authors and do not necessarily represent those of their affiliated organizations, or those of the publisher, the editors and the reviewers. Any product that may be evaluated in this article, or claim that may be made by its manufacturer, is not guaranteed or endorsed by the publisher.

- Peccerillo, A., Donati, C., Santo, A., Orlando, A., Yirgu, G., and Ayalew, D. (2007). Petrogenesis of silicic peralkaline rocks in the Ethiopian rift: Geochemical evidence and volcanological implications. *J. Afr. Earth Sci.* 48 (2), 161–173. doi:10.1016/j.jafrearsci.2006.06.010
- Raggiunti, M., Keir, D., and Pagli, C. (2021). Mapping hydrothermal alteration at the fentale-dofan magmatic segment of the Main Ethiopian rift. *Front. Earth Sci.* 9, 716144. doi:10.3389/feart.2021.716144
- Reimer, P. J., Bard, E., Bayliss, A., Beck, J. W., Blackwell, P. G., Ramsey, C. B., et al. (2013). IntCal13 and Marine13 radiocarbon age calibration curves 0–50,000 Years cal BP. *Radiocarbon* 55, 1869–1887. doi:10.2458/azu\_js\_rc.55.16947
- Ronga, F., Lustrino, M., Marzoli, A., and Melluso, L. (2010). Petrogenesis of a basalt-comendite-pantellerite rock suite: The boseti volcanic complex (Main Ethiopian rift). *Mineral. Pet.* 98, 227–243. doi:10.1007/s00710-009-0064-3
- Rooney, T., Bastow, I. D., and Keir, D. (2011). Insights into extensional processes during magma assisted rifting: Evidence from aligned scoria cones. *J. Volcanol. Geotherm. Res.* 201, 83–96. doi:10.1016/j.jvolgeores.2010.07.019
- Rooney, T., Furman, T., Bastow, I., Ayalew, D., and Yirgu, G. (2007). Lithospheric modification during crustal extension in the Main Ethiopian Rift. *J. Geophys. Res.* 112, B10201. doi:10.1029/2006JB004916
- Ruch, J., Keir, D., Passarelli, L., Di Giacomo, D., Ogubazghi, G., and Jónsson, S. (2021). Revealing 60 years of earthquake swarms in the southern Red Sea, Afar and the Gulf of Aden. *Front. Earth Sci.* 9, 664673. doi:10.3389/feart.2021.664673
- Siegburg, M., Bull, J. M., Nixon, C. W., Keir, D., Gernon, T. M., Corti, G., et al. (2020). Quantitative constraints on faulting and fault slip rates in the northern Main Ethiopian Rift. *Tectonics* 39, e2019TC006046. doi:10.1029/2019TC006046
- Siegburg, M., Gernon, T. M., Bull, J. M., Keir, D., Barfod, D. N., Taylor, R. N., et al. (2018). Geological evolution of the boset-bericha volcanic complex, Main Ethiopian rift:  $^{40}\text{Ar}/^{39}\text{Ar}$  evidence for episodic pleistocene to Holocene volcanism. *J. Volcanol. Geotherm. Res.* 351, 115–133. doi:10.1016/j.jvolgeores.2017.12.014
- Sigmundsson, F., Hooper, A., Hreinsdóttir, S., Vogfjörð, K. S., Ófeigsson, B. G., Heimisson, E. R., et al. (2015). Segmented lateral dyke growth in a rifting event at Bárðarbunga volcanic system, Iceland. *Nature* 517, 191–195. doi:10.1038/nature14111
- Sigmundsson, F., Parks, M., Hooper, A., Geirsson, H., Vogfjörð, K. S., Drouin, V., et al. (2022). Deformation and seismicity decline before the 2021 Fagradalsfjall eruption. *Nature* 609, 523–528. doi:10.1038/s41586-022-05083-4
- Sun, S. S., and McDonough, W. F. (1989). Chemical and isotopic systematics of oceanic basalts: Implications for mantle composition and processes. *Geol. Soc. Lond. Spec. Publ.* 42, 313–345. doi:10.1144/gsl.sp.1989.042.01.19
- Temtime, T., Biggs, J., Lewi, E., and Ayele, A. (2020). Evidence for active rhyolitic dike intrusion in the northern Main Ethiopian Rift from the 2015 Fentale seismic swarm. *Geochem. Geophys. Geosystems* 21, e2019GC008550. doi:10.1029/2019GC008550
- Viltres, R., Jónsson, S., Ruch, J., Doubre, C., Reilinger, R., Floyd, M., et al. (2020). Kinematics and deformation of the southern Red Sea region from GPS observations. *Geophys. J. Int.* 221, 2143–2154. doi:10.1093/gji/ggaa109
- Wadge, G., Biggs, J., Lloyd, R., and Kendall, J. M. (2016). Historical volcanism and the state of stress in the East African Rift system. *Front. Earth Sci.* 4, 86. doi:10.3389/feart.2016.00086
- Williams, F. M. (2016). *Understanding Ethiopia: Geology and scenery*. Cham: Springer, 343. doi:10.1007/978-3-319-02180-5\_2759
- Williams, F., Williams, M., and Aumento, F. (2004). Tensional fissures and crustal extension rates in the northern part of the Main Ethiopian Rift. *J. Afr. Earth Sci.* 38, 183–197. doi:10.1016/j.jafrearsci.2003.10.007
- Wooley, A. R. (2001). *Alkaline rocks and carbonatites of the world: Africa*. London: Geological Society of London, 372.
- Wright, T. J., Ebinger, C., Biggs, J., Ayele, A., Yirgu, G., Keir, D., et al. (2006). Magma-maintained rift segmentation at continental rapture in the 2005 Afar dyking episode. *Nature* 442, 291–294. doi:10.1038/nature04978